

Sympathetic cooling of an atomic Bose-Fermi gas mixture

W. Geist, L. You, and T. A. B. Kennedy

School of Physics, Georgia Institute of Technology, Atlanta, Georgia 30332-0430

(Received 18 August 1998)

Sympathetic cooling of an atomic Fermi gas by a Bose gas is studied by solution of the coupled quantum Boltzmann equations for the confined gas mixture. Results for equilibrium temperatures and relaxation dynamics are presented, and some simple models are developed. Our study illustrates that a combination of sympathetic and forced evaporative cooling enables the Fermi gas to be cooled to the degenerate regime where quantum statistics and mean-field effects are important. The influence of mean-field effects on the equilibrium spatial distributions is discussed qualitatively. [S1050-2947(99)03402-2]

PACS number(s): 03.75.Fi, 05.30.Fk, 05.30.Jp, 05.20.Dd

I. INTRODUCTION

The magnetic trapping and forced evaporative cooling of alkali-metal vapors has led to the Bose-Einstein condensation of a number of different atomic species [1]. As a consequence, the many-body physics of confined, weakly interacting Bose gases are now amenable to experimental investigation. To date, most experimental and theoretical research on degenerate atomic gases has focused on bosons [2]. Recently, some exotic systems have been investigated experimentally. These include the Bose condensation of spin mixtures of ^{87}Rb using sympathetic cooling [3] and a report of spin domains of ^{23}Na in an optical trap [4]. There is now a growing interest in the properties of degenerate atomic Fermi gases [5–11] and boson-fermion mixtures [12], although to date a degenerate atomic Fermi gas has not been achieved.

In this paper we investigate the process of sympathetic cooling of an initially nondegenerate Fermi gas to the quantum degenerate regime using a Bose gas as a coolant. Sympathetic cooling of a Fermi gas to degeneracy is necessary as a result of the suppression of s -wave scattering between identical fermions in spin symmetric states. Evaporative cooling of a pure fermion gas trapped in a single hyperfine state, which depends on rethermalization through atomic collisions, is thus ineffective at temperatures sufficiently low that only the lowest few partial waves contribute. The Fermi gas may instead be cooled by thermal contact with a cold Bose gas, which may be either already condensed before thermal contact with the Fermi gas or evaporatively cooled in its presence. We investigate the dynamics using the quantum Boltzmann equation (QBE) for the Bose-Fermi gas mixture. The QBE has been applied to describe the population dynamics for a Bose gas by a number of authors who solved it by direct integration [13,14], trajectory simulation [15], and Bird's simulation method [16]. The first two sets of authors make the assumption that the distribution is ergodic at all times [17] to simplify the numerical computation, whereas in Bird's method collision dynamics are constructed from simulated particle trajectories. In this paper we solve the QBE in the ergodic approximation by direct integration of the coupled differential equations which describe the Fermi and Bose gas distribution functions.

We consider a harmonically trapped gas of N_f fermions

with Fermi temperature given by $E_F \equiv k_B T_F = \hbar \omega (6N_f)^{1/3}$, which is in thermal contact with a similarly confined gas of N_b bosons with condensation temperature $k_B T_C = \hbar \omega (N_b/1.202)^{1/3}$. By evaporatively cooling the Bose gas through T_C down to a temperature ηT_C ($0 < \eta < 1$), the Fermi gas will equilibrate to the Fermi temperature provided $N_f < \eta^3 N_C / 7.212$, where $N_C < N_b$ is the number of condensed atoms remaining. Solution of the QBE gives both the energy and spatial distributions of the Bose and Fermi gases. An important limitation of our present treatment is the neglect of mean-field effects on the dynamics. These are potentially important when the Bose and Fermi gas are degenerate and the mean-field energy exceeds the trap frequency. In a recent paper, Mølmer [12] used a simple mean-field model to study the spatial distributions of a Bose-Fermi gas mixture at $T=0$ K. The distributions depend strongly on the relative sign and magnitude of the boson-boson and boson-fermion scattering lengths. A complete and numerically tractable approach to quantum kinetics, which incorporates such mean-field effects in addition to the population dynamics, is still under investigation. A qualitative discussion of the influence of mean-field effects on our results is given in Sec. IV.

The remainder of this paper is organized as follows. In Sec. II we discuss the equilibrium temperatures for an initially hot Fermi gas placed in thermal contact with a cold Bose gas. We also derive a simple dynamical model for the thermalization using the assumption that both gases are described by a Maxwell-Boltzmann distribution at all times. In Sec. III we describe a theoretical model based on the QBE for the Fermi-Bose mixture and the treatment of forced evaporative cooling. In Sec. IV we present results of solutions of the QBE which provide information on the kinetic temperature and spatial distributions of the mixture. Using recent atomic data we also present some results for the sympathetic cooling of the $^{40}\text{K}/^{39}\text{K}$ Fermi/Bose potassium isotopes. Finally, in Sec. V, we summarize our conclusions.

II. EQUILIBRIUM PROPERTIES AND COOLING WITHOUT FORCED EVAPORATION

A. Equilibrium temperature

If two gases at different initial temperatures are brought into contact, they will rethermalize to a common equilibrium

temperature which can be obtained using conservation of particle number and energy (overbar indicates average energy),

$$\bar{\epsilon}_{\text{tot}} = \bar{\epsilon}_f(0) + \bar{\epsilon}_b(0) = \bar{\epsilon}_f(\infty) + \bar{\epsilon}_b(\infty), \quad (1)$$

assuming that there are no losses during relaxation. For a Bose-Fermi gas mixture the equilibrium temperature T_∞ can be found numerically using the Bose-Einstein and Fermi-Dirac distribution functions as follows. Given the number of bosons N_b and fermions N_f , and the initial temperatures $T_b(0)$ and $T_f(0)$ we set $T_f = T_b$ at each iteration step and compute the fugacity z_f for the Fermi gas by solving

$$N_f = \sum_{\epsilon_i} g(\epsilon_i) (z_f^{-1} e^{\epsilon_i/k_B T_f} + 1)^{-1}, \quad (2)$$

with $g(\epsilon_i)$ the degeneracy of states with energy ϵ_i . We then compute the mean energy $\bar{\epsilon}_f(z_f, T_f)$ for the Fermi gas and determine T_b and z_b for the Bose gas by the following iteration: set $\bar{\epsilon}_b = \bar{\epsilon}_{\text{tot}} - \bar{\epsilon}_f(z_f, T_f)$ and compute T_b from

$$\bar{\epsilon}_b = \sum_{\epsilon_i} \epsilon_i g(\epsilon_i) (z_b^{-1} e^{\epsilon_i/k_B T_b} - 1)^{-1}. \quad (3)$$

Then compute z_b by solving

$$N_b = \sum_{\epsilon_i} g(\epsilon_i) (z_b^{-1} e^{\epsilon_i/k_B T_b} - 1)^{-1} \quad (4)$$

and repeat this iteration until $[N_b(z_b, T_b) - N_b]/N_b < 10^{-7}$ and $[\bar{\epsilon}_b(z_b, T_b) - \bar{\epsilon}_b]/\bar{\epsilon}_b < 10^{-7}$. We then set $T_f = T_b$ and repeat the procedure until $(T_f - T_b)/T_f < 10^{-4}$.

For temperatures $T_f \geq 0.5T_F$ and $T_\infty < T_C$ an approximate equation can be obtained using a classical Maxwell-Boltzmann distribution for the Fermi gas and a Bose distribution with $z_b = 1$ for the Bose gas. This yields

$$g_4(1) \frac{T_\infty^4}{T_F^4} + \frac{T_\infty}{6T_F} = g_4(1) \frac{T_b(0)^4}{T_F^4} + \frac{T_f(0)}{6T_F}, \quad (5)$$

with the Bose-Einstein function $g_4(1) \approx 1.082$. If $T_\infty > T_C$, we can approximate the Bose-Einstein distribution with a Maxwell-Boltzmann distribution to obtain an explicit expression for the temperature,

$$T_\infty = \frac{N_f T_f(0) + N_b T_b(0)}{N_f + N_b}. \quad (6)$$

In Fig. 1 we show the equilibrium temperature as a function of the initial Fermi gas temperature scaled in units of T_F . The Bose gas consists of 10^6 atoms at initial temperature $T_b(0) = 0.1T_f(0)$, where T_F depends on the number of fermions, which is varied between 10^4 and 10^6 . In terms of the BEC temperature, the initial temperature of the Bose gas lies in the range $0.02T_C < T_b(0) < 0.2T_C$. The full numerical results agree well with approximation Eq. (5) for $N_f = 10^3, 10^4$, and 10^5 in the temperature range considered. This is shown by the curves at the bottom of the figure, which almost overlap the approximate solution. The equilibrium temperature T_∞ stays below the critical temperature T_C

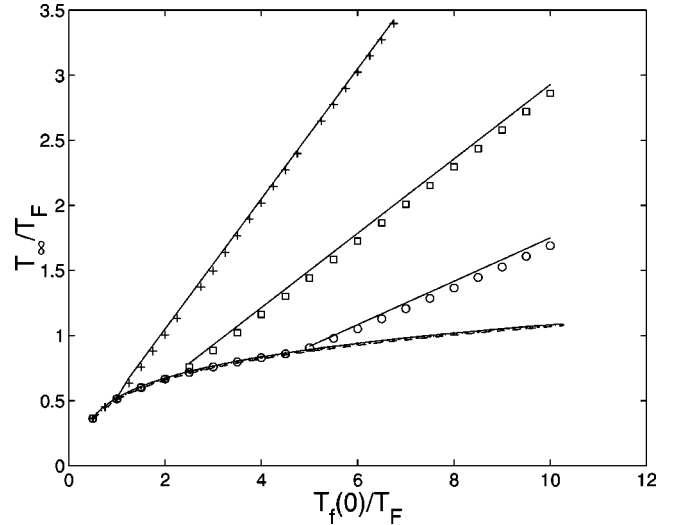


FIG. 1. Equilibrium temperature as a function of the initial Fermi gas temperature in units of T_F . The number of fermions is $N_f = 10^3$ (—), $N_f = 10^4$ (---), $N_f = 10^5$ (···), $N_f = 2 \times 10^5$ (○), $N_f = 4 \times 10^5$ (◇), $N_f = 10^6$ (+). The solid lines show the results using Eq. (5) and Eq. (6), respectively. The number of bosons is $N_b = 10^6$ and the initial temperature is always chosen as $\bar{T}_b(0) = 0.1\bar{T}_F$ corresponding to $\bar{T}_b(0) = 0.019\bar{T}_C, 0.042\bar{T}_C, 0.09\bar{T}_C, 0.13\bar{T}_C, 0.142\bar{T}_C$, and $0.19\bar{T}_C$.

and, in agreement with Eq. (5), T_∞/T_F does not depend on the number of fermions. If we increase the number of fermions or alternatively the initial Fermi gas temperature, the Bose gas will be heated above T_C and the equilibrium temperature shows the linear dependence on $T_f(0)$ as derived in Eq. (6). From our numerical studies we find that Fermi statistics become significant only for $T_f \lesssim 0.5T_F$ (see also [18]), which in general can be reached with additional evaporative cooling of the gas mixture.

B. Thermalization of a two-component mixture

We consider Bose and Fermi gases brought into thermal contact in a confining potential, at different initial temperatures $T_b(0)$ and $T_f(0)$, respectively. We are primarily interested here in a regime prior to a stage of forced evaporative cooling, in which the Bose gas as well as the Fermi gas are nondegenerate. The thermalization may result in a significant alteration in the energy and spatial distribution of fermionic atoms in the trap. A simple dynamical description of the thermalization can be derived using the classical Boltzmann equation in the ergodic approximation. The mean energy of component $k = (b, f)$ is given by

$$\bar{\epsilon}_k(t) = \int \epsilon \mathcal{F}_k(\epsilon, t) \rho(\epsilon) d\epsilon, \quad (7)$$

where $\mathcal{F}_k(\epsilon, t)$ is the ergodic distribution function for component k and $\rho(\epsilon) = \epsilon^2/2(\hbar\omega)^3$ is the density of states for a harmonic trap of mean frequency $\omega = (\omega_x \omega_y \omega_z)^{1/3}$. For simplicity, we assume that both components see the same trapping potential.

The time dependence of the energy of the Fermi gas is then obtained by integrating the Boltzmann equation [13] over all energies,

$$\frac{d\bar{E}_f}{dt} = \frac{1}{\tau_0} \frac{1}{(\hbar\omega)^5} \int dE_1 \int dE_2 \int dE_3 \int dE_4 E_{\min}^2 / 2E_1 \delta(E_1 + E_2 - E_3 - E_4) [\mathcal{F}_f(E_4, t) \mathcal{F}_b(E_3, t) - \mathcal{F}_f(E_2, t) \mathcal{F}_b(E_1, t)], \quad (8)$$

where all energies written with upper case E are dimensionless, i.e., $E \equiv \epsilon/\hbar\omega$, $E_{\min} \equiv \min\{E_1, E_2, E_3, E_4\}$, and the natural time scale τ_0 is given in terms of the Bose-Fermi s -wave collision cross section σ_{bf} by $1/\tau_0 \equiv (\hbar\omega)^2 m \sigma_{bf} / \pi^2 \hbar^3$. We have dropped the term which represents collisions between fermionic atoms assuming that the p -wave contribution is negligible at the low energies under consideration.

To get some qualitative insight into the thermalization dynamics, we need to further simplify the model. We assume that the component distribution functions are Boltzmann-like at all times, and parametrized by time-dependent fugacity $z_k(t)$ and dimensionless temperature $\bar{T}_k(t) \equiv k_B T_k(t) / \hbar\omega$ as follows:

$$\mathcal{F}[E, z_k(t), \bar{T}_k(t)] = z_k(t) e^{-E/\bar{T}_k(t)}. \quad (9)$$

The average energy and particle number for a trapped Maxwell-Boltzmann distribution are given by

$$\bar{E}_k = \frac{z_k \bar{T}_k^4}{2} \int dx x^3 e^{-x}, \quad (10)$$

$$N_k = \frac{z_k \bar{T}_k^3}{2} \int dx x^2 e^{-x} \quad (11)$$

from which it follows that $z_k = N_k / \bar{T}_k^3$ and $\bar{E}_k = 3N_k \bar{T}_k$. The fugacity of component k can therefore be eliminated in terms of the particle number and mean energy. Another simplification which results from the approximation is that the scattering of two bosons does not alter the average energy of the Bose gas.

It is convenient to write the average energy in terms of a dimensionless temperature, thus

$$\begin{aligned} \frac{d\bar{T}_f}{dt} &= \frac{N_b r^3}{3\tau_0} \int dx_1 \int dx_2 \int dx_3 \int dx_4 \frac{x_{\min}^2}{2} \\ &\quad \times x_1 \delta(x_1 + x_2 - x_3 - x_4) (e^{-x_4} e^{-rx_3} - e^{-x_2} e^{-rx_1}) \\ &= \frac{N_b}{3\tau_0} P(T_f/T_b), \end{aligned} \quad (12)$$

$$\frac{d\bar{T}_b}{dt} = -\frac{N_f}{3\tau_0} P(T_f/T_b), \quad (13)$$

where $r \equiv \bar{T}_f/\bar{T}_b$, and the rational function

$$P(r) = \frac{1 + 3r + 2r^2 - 2r^3 - 3r^4 - r^5}{(1+r)^5}. \quad (14)$$

The equilibrium temperature \bar{T}_∞ is obtained from $d\bar{T}_f/d\bar{T}_b = -N_b/N_f$. Integrating from $t=0$ to ∞ , we recover Eq. (6).

The analysis shows that the time scale for relaxation is approximately $\bar{T}_b \tau_0 / N_f$. In Fig. 2 we compare the predictions of this simple dynamical model, with the full dynamics of the QBE as discussed in the following section. The solutions show that the time scale that describes equilibration is on the order of $\tau_r \equiv \bar{T}_b \tau_0 / N_f \approx 0.043 \tau_0$, as predicted by Eqs. (12) and (13).

If forced evaporative cooling is applied to the gas mixture, atoms from the hot energy tail are removed. The rate of evaporation must be chosen to be much smaller than the relaxation rate of the gas, as discussed above. Another way to determine the relaxation time is to calculate the initial mean collision rate γ using the Boltzmann collision integral. Consider the collisions of a ‘‘test’’ atom, with energies E_1 , with atoms of energy E_2 , into final states with energies E_3 and E_4 . One sums over all initial energies E_1 , and divides by the number of particles to get the energy averaged rate per particle,

$$\begin{aligned} \gamma(\bar{T}, N) &= \frac{1}{\tau_0} \frac{N}{\bar{T}} \int dx_1 dx_2 dx_3 dx_4 \delta(x_1 + x_2 - x_3 - x_4) \\ &\quad \times \frac{x_{\min}^2}{2} e^{-x_1} e^{-x_2} = \frac{N}{2\tau_0 \bar{T}}, \end{aligned} \quad (15)$$

in qualitative agreement with the simple model above. We note, however, that the relaxation rate we have discussed here should not be regarded as the characteristic time scale for condensation [19–21].

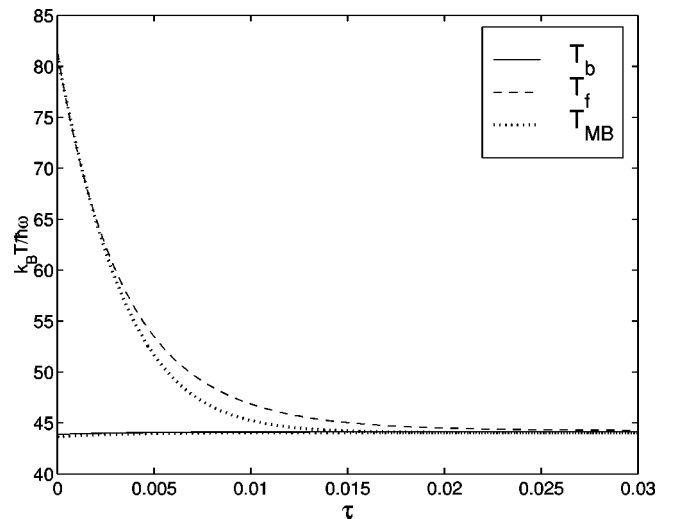


FIG. 2. The temperature of the Bose gas (solid line) and of the Fermi gas (broken line) as a function of time. The dotted line denotes the temperature obtained by solving the differential equations assuming a Maxwell-Boltzmann distribution with time-dependent fugacity and temperature.

III. QUANTUM BOLTZMANN EQUATION AND FORCED EVAPORATION

A. Quantum Boltzmann equation

The QBE for a harmonically confined Bose gas has been discussed elsewhere within the ergodic approximation [15,22]. The QBE for an interacting two-component Bose-Fermi mixture in the harmonic trap can be written ($\tau = t/\tau_0$)

$$\begin{aligned}
 g(E_i) \frac{db_{E_i}}{d\tau} &= \alpha_b \sum_{E_j, E_k, E_l} \delta_{E_i+E_j, E_k+E_l} g(E_i, E_j, E_k, E_l) \\
 &\times [b_{E_k} b_{E_l} (1+b_{E_j})(1+b_{E_i}) \\
 &- b_{E_i} b_{E_j} (1+b_{E_k})(1+b_{E_l})] \\
 &+ \sum_{E_j, E_k, E_l} \delta_{E_i+E_j, E_k+E_l} g(E_i, E_j, E_k, E_l) \\
 &\times [b_{E_k} f_{E_l} (1-f_{E_j})(1+b_{E_i}) \\
 &- b_{E_l} f_{E_j} (1-f_{E_l})(1+b_{E_i})], \quad (16)
 \end{aligned}$$

$$\begin{aligned}
 g(E_i) \frac{df_{E_i}}{d\tau} &= \alpha_f \sum_{E_j, E_k, E_l} \delta_{E_i+E_j, E_k+E_l} g(E_i, E_j, E_k, E_l) \\
 &\times [f_{E_k} f_{E_l} (1-f_{E_j})(1-f_{E_i}) \\
 &- f_{E_l} f_{E_j} (1-f_{E_k})(1-f_{E_i})] \\
 &+ \sum_{E_j, E_k, E_l} \delta_{E_i+E_j, E_k+E_l} g(E_i, E_j, E_k, E_l) \\
 &\times [b_{E_l} f_{E_k} (1-f_{E_i})(1+b_{E_j}) \\
 &- b_{E_j} f_{E_l} (1-f_{E_k})(1+b_{E_i})], \quad (17)
 \end{aligned}$$

where b_n and f_n are the number of Bose and Fermi atoms in state E_n . The collision matrix elements are approximately given by

$$g(E_i, E_j, E_k, E_l) = g(E_{\min}), \quad (18)$$

with $g(E_n)$ the degeneracy of energy level E_n , and E_{\min} is the minimum energy of all four energies involved in the scattering process, as defined earlier. Although this approximation is not quantitatively accurate for the lowest several states of the trap, it is sufficient to illustrate the main qualitative features of sympathetic cooling. In an isotropic trap the degeneracy of the energy state $\epsilon_n = \hbar\omega(n-1)$, $n = 1, 2, \dots$, is $g(E_n) = n(n+1)/2$. The coefficients $\alpha_b = \sigma_{bb}/\sigma_{bf}$ and $\alpha_f = \sigma_{ff}/\sigma_{bf}$ give the ratios of the cross sections for boson-boson and fermion-fermion scattering, respectively, to the boson-fermion cross section. Exchange symmetry leads to $\alpha_f = 0$ since the s -wave cross section vanishes for identical fermions. Of course, this is the reason we must employ sympathetic cooling with a Bose gas refrigerant.

B. Forced evaporative cooling

Evaporative cooling in magnetic traps is performed by inducing transitions to untrapped states with a radio-frequency field. This is modeled here by the following procedure. Particles that are scattered into states with energy larger than the time-varying cutoff energy $E_{\text{cut}}(\tau)$ are lost. The latter is a given decreasing function of time in the case of forced evaporative cooling. A particle may be scattered into a state with energy $E_i < E_{\text{cut}}(\tau)$ by two-body scattering of atoms in states with energies E_k and E_l , i.e., $E_k, E_l \rightarrow E_i, E_j$, in which $E_j > E_{\text{cut}}(\tau)$, so that one particle is lost from the trap. Similarly a particle in energy level E_i can be scattered out of this energy level, $E_i, E_j \rightarrow E_k, E_l$, resulting in one particle loss from the trap when either $E_k > E_{\text{cut}}(\tau)$ or $E_l > E_{\text{cut}}(\tau)$. Explicitly, we have the following

(a) The gain process for energy level E_i ,

$$\begin{aligned}
 g(E_i) \frac{dn_{E_i}}{d\tau} &= \alpha \sum_{E_j > E_{\text{cut}}(\tau) > E_k, E_l}^{E_j < 2E_{\text{cut}}(\tau)} \delta_{E_i+E_j, E_k+E_l} g(E_i, E_j, E_k, E_l) \\
 &\times n_{E_k} n_{E_l} (1 \pm n_{E_i}). \quad (19)
 \end{aligned}$$

(b) The loss process for energy level E_i ,

$$\begin{aligned}
 g(E_i) \frac{dn_{E_i}}{d\tau} &= -2\alpha \sum_{E_k > E_{\text{cut}}(\tau) > E_j, E_l}^{E_k < 2E_{\text{cut}}(\tau)} \delta_{E_i+E_j, E_k+E_l} g(E_i, E_j, E_k, E_l) \\
 &\times n_{E_i} n_{E_j} (1 \pm n_{E_l}), \quad (20)
 \end{aligned}$$

where n_{E_i} denotes the distribution function for Fermi or Bose atoms with energy E_i , as appropriate.

The kinetics of forced evaporative cooling is modeled by adding these terms to the QBE, Eqs. (16) and (17), which include all two-body collision processes between initial and final states i, j, k , and l with energies $E_i, E_j, E_k, E_l < E_{\text{cut}}(\tau)$ conserving the total number of particles in the trap.

IV. RESULTS AND DISCUSSION

In this section we illustrate the dynamics of sympathetic cooling of Bose-Fermi gas mixtures, through their energy, state, and spatial distribution functions. The spatial distributions of confined degenerate Bose and Fermi atomic gases are quite different. An ideal Bose condensate has a size determined by the quantum width of the trap ground state $l = \sqrt{\hbar/2M\omega}$, whereas the size of a Fermi gas is governed by the Fermi width $R_F = (E_F/2M\omega^2)^{1/2}$, which scales as $R_F \sim N_f^{1/6} l$, as a result of the Pauli exclusion principle. For an interacting Bose gas, with positive scattering length, the condensate is larger than l , and for strongly condensed gases its size can be estimated using mean-field theory in the Thomas-Fermi approximation [23]. Mean-field effects, which can be significant well below the condensation temperature, are not included in our model. These may be important in the final stages of cooling if the Bose gas is already strongly condensed at this stage. Our illustrations of the spatial distributions of both Fermi and Bose gas employ the universal scal-

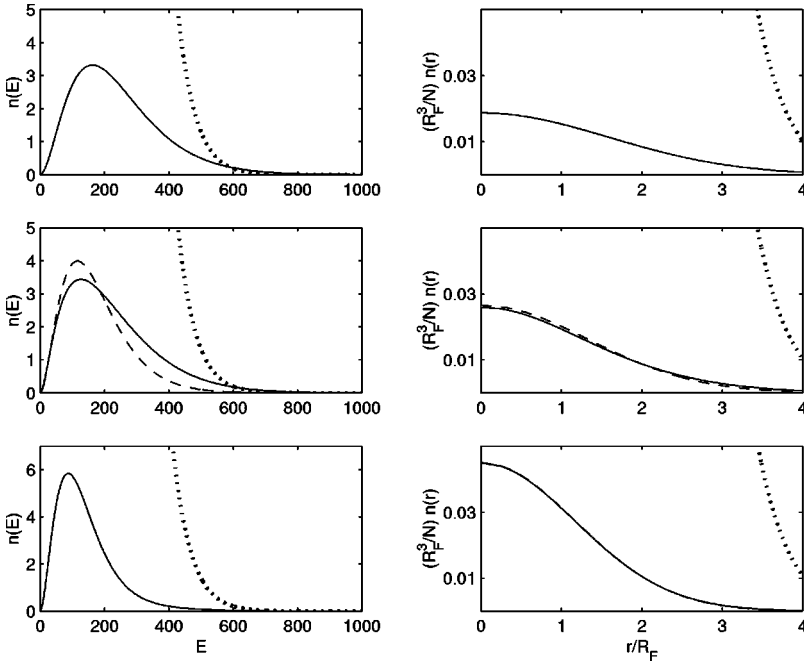


FIG. 3. The Fermi (solid line) and Bose (dotted line) distribution functions at times $\tau = 0, 0.003$ and 0.016 . The graphs on the left show the number of atoms as a function of energy and the graphs on the right show the spatial distribution. Initial conditions are $N_b(0) = 10^5$, $N_f(0) = 10^3$, $\bar{T}_b(0) = \bar{T}_C = 43.7$, and $\bar{T}_f(0) = 5\bar{T}_F = 81.8$. Both gases are in contact at $\tau=0$ and then relax to the equilibrium temperature $\bar{T}_\infty = 44$. The broken lines denote the fit to the Fermi distribution and coincide with full lines at $\tau=0$ and $\tau = 0.016$.

ing described by Butts and Rokhsar [18], who showed that for a harmonically trapped ideal Fermi gas at $T=0$,

$$n_f(r) = \frac{N_f}{R_F^3} \frac{8}{\pi^2} \left[1 - \left(\frac{r}{R_F} \right)^2 \right]^{3/2}. \quad (21)$$

It should be remembered that with evaporative cooling the number of fermionic and bosonic atoms is a time-dependent variable, and therefore so is R_F . In the figures we always scale with respect to the instantaneous value of R_F .

In Figs. 2 and 3 we present the rethermalization of a nondegenerate Fermi gas immediately after it is placed in thermal contact with a Bose gas which is initially at the Bose condensation temperature T_C . The calculation is performed by numerical integration of the QBE without any forced evaporative cooling. In Fig. 3 the temperature of the Fermi

gas alters considerably over a time scale $\tau_0 \bar{T}_f / N_b$ [Eq. (12)]. Initially a hot tail of atoms extends to the trap extremities and during the early stages of equilibration the Fermi gas distribution deviates significantly from a Fermi-Dirac distribution which fits the average energy and particle number. The gas then equilibrates to a nondegenerate state as can be seen from inspection of the peak of the spatial distribution function, $n_f(r=0) \ll 1$ [18]. The Bose gas has one hundred times more particles than the Fermi gas, and completely envelops the Fermi gas at all times. Figure 2 compares the simple model of thermalization discussed in the preceding section with the QBE. The model is very good in the early stages, but the agreement deteriorates in the intermediate regime before steady state is achieved.

In Figs. 4 and 5 we consider the forced evaporative cooling of both gases. In contrast to Figs. 2 and 3, there are 10^5

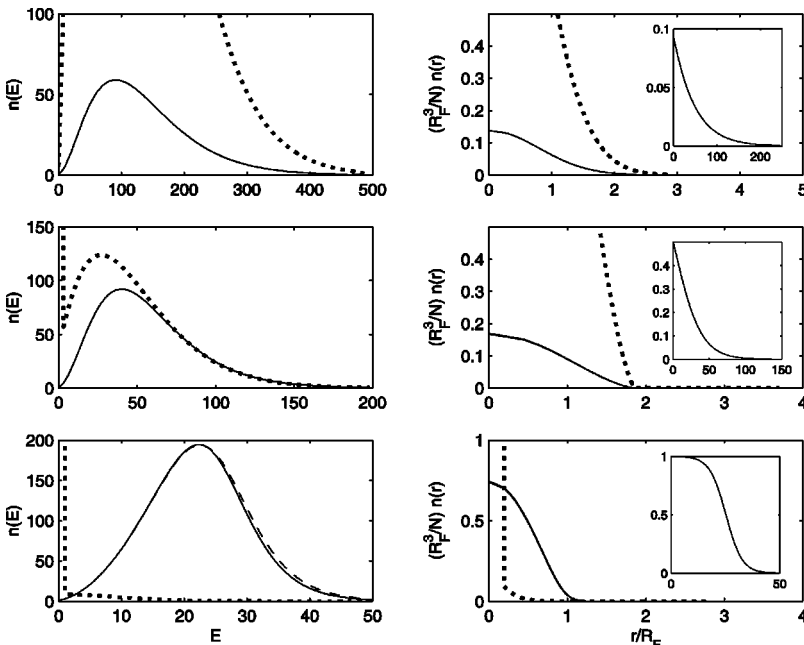


FIG. 4. The Fermi (solid line) and Bose (dotted line) distribution functions at times $\tau = 0, 0.9$, and 2.0 . The graphs on the left show the number of atoms as a function of energy, the graphs on the right show the spatial distribution, and the inset shows the number of fermions per energy divided by the degeneracy. Initial conditions are $N_b(0) = 10^5$, $N_f(0) = 10^4$, $\bar{T}_b(0) = \bar{T}_C = 43.7$, $\bar{T}_f(0) = 5\bar{T}_F = 186$. From $\tau=0$ until $\tau=0.04$ the cutoff for the Bose gas is $E_{\text{cut}} = 500$ and for the Fermi gas $E_{\text{cut}} = 1000$. After $\tau=0.04$ the cutoff energy is ramped down with a rate $\gamma = 1.0$ for both gases starting at $E_0 = 500$. [$E_{\text{cut}}(\tau) = e^{-\gamma\tau} E_0$.] The fit to the Fermi distribution is also drawn as a broken line. The temperatures from top to bottom are $\bar{T}_f(\tau) = 5\bar{T}_F$, $0.6\bar{T}_F$, $0.14\bar{T}_F$ and $\bar{T}_b(\tau) = \bar{T}_C$, $0.5\bar{T}_C$, $0.1\bar{T}_C$.

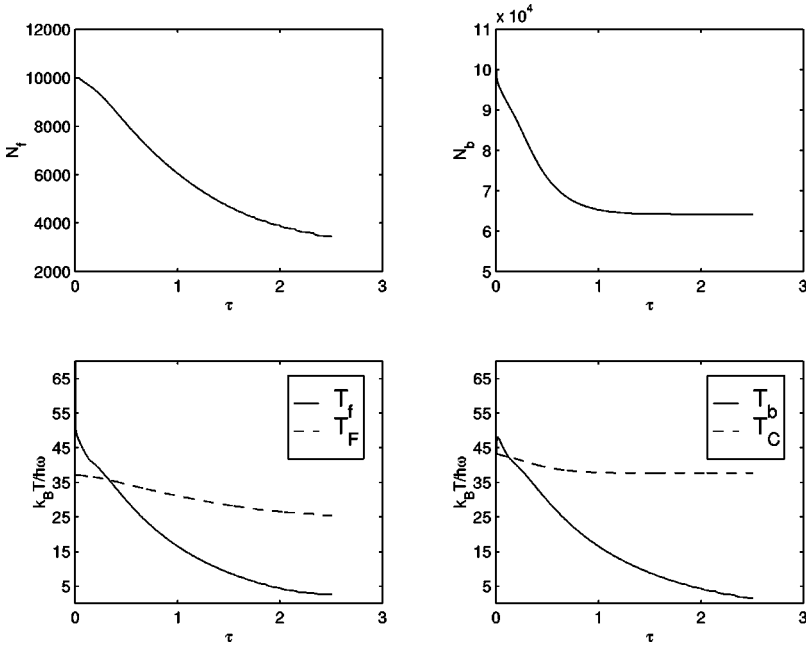


FIG. 5. Upper graph: the number of bosons and fermions remaining in the trap. Lower graph: the temperature of the gases as a function of time. The dotted lines show the critical temperature for the Bose gas and the Fermi temperature.

bosons and 10^4 fermions, initially. The forced cooling begins after the initial equilibration stage during which the boson temperature increases (Fig. 5), following thermal contact of the two gases. The evaporative cooling time scale is chosen to be τ_0 , which is much longer than both the relaxation time scale of the one-component Bose gas [Eq. (15)] and the relaxation time scale of the Fermi gas with the Bose gas [Eq. (12)]. The Bose gas energy distribution shows the formation of the condensate and the corresponding spatial distribution contracts to that of the condensate with a small thermal component. The degenerate Fermi gas is then exposed and its spatial distribution is close to the zero-temperature limit [Eq. (21)], which has a maximum density at the trap center $n_f(0)R_F^3/N_f = 8/\pi^2 \approx 0.81$. The inset shows the state occupancy for the Fermi distribution with the characteristic smearing of the Fermi surface at finite temperature, and near

unit occupancy for low-lying levels. It is interesting to note that evaporative cooling of the Fermi gas still proceeds at later times when the spatial overlap between fermions and bosons is mainly in a small region at the center of the trap where the condensate is located. The collisions which result in cooling involve orbits of hot fermions through the trap center where they collide with cold condensed bosons. At this stage evaporation mainly results in depletion of fermions as can be seen in Fig. 5. We also simulate the case when the evaporative cooling involves only the loss of Bose atoms from the trap. In Figs. 6 and 7 we consider the same initial conditions as for Figs. 4 and 5, but only ramp down the cutoff energy for the bosons. The results are qualitatively the same as in the former case where both Bose and Fermi gas particles evaporate, except that we end up with more particles left in the Fermi gas. As mentioned earlier, we have

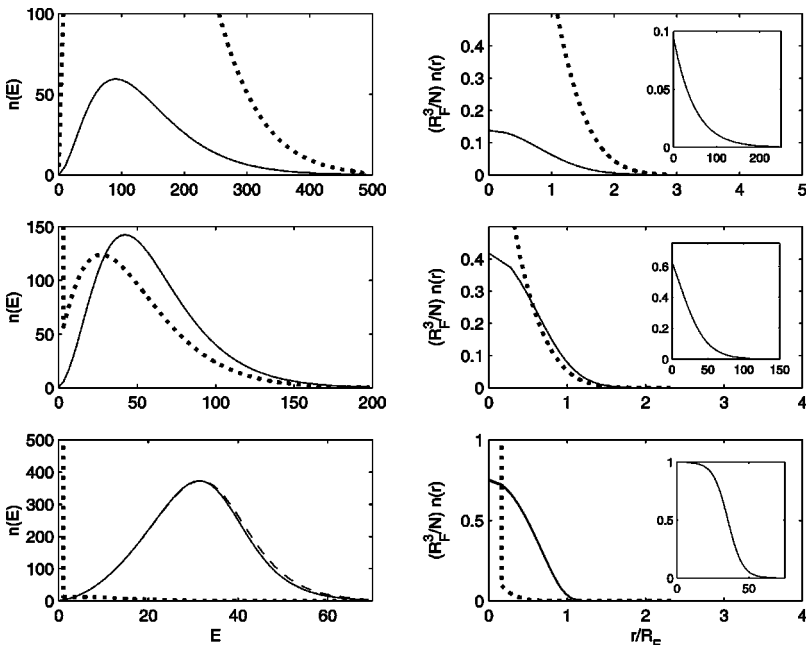


FIG. 6. The Fermi (solid line) and Bose (dotted line) distribution functions at times $\tau=0, 0.9$, and 2.2 . The graphs on the left show the number of atoms as a function of energy, the graphs on the right show the spatial distribution, and the inset shows the number of fermions per energy divided by the degeneracy. Initial conditions are $N_b(0) = 10^5$, $N_f(0) = 10^4$, $\bar{T}_b(0) = \bar{T}_C = 43.7$, $\bar{T}_f(0) = 5\bar{T}_F = 186$. From $\tau=0$ until $\tau=0.04$ the cutoff for the Bose gas is $E_{b\text{cut}} = 500$ and for the Fermi gas $E_{f\text{cut}} = 1000$. After $\tau=0.04$, the cutoff energy is ramped down with a rate $\gamma = 1.0$ only for the Bose gas starting at $E_0 = 500$. [$E_{\text{cut}}(\tau) = e^{-\gamma\tau}E_0$.] The fit to the Fermi distribution is also drawn as a broken line. The temperatures from top to bottom are $\bar{T}_f(\tau) = 5\bar{T}_F$, $0.5\bar{T}_F$, $0.14\bar{T}_F$ and $\bar{T}_b(\tau) = \bar{T}_C$, $0.5\bar{T}_C$, $0.14\bar{T}_C$.

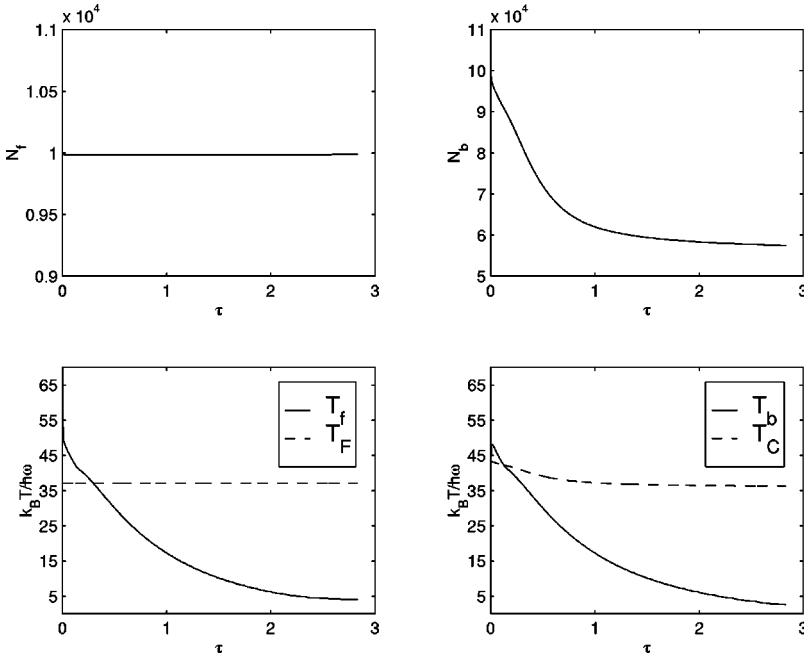


FIG. 7. Upper graph: The number of bosons and fermions remaining in the trap. Lower graph: the temperature of the gases as a function of time. The dashed lines show the critical temperature for the Bose gas and the Fermi temperature.

not included the effect of the bosonic mean-field which can alter the spatial distributions of each component depending on the mean field strength, the ratio of the scattering lengths, and the particle numbers of both components [12].

A possible experimental scenario for sympathetic cooling of a Bose-Fermi mixture involves two isotopes of potassium. Recent calculations predict the s -wave scattering length for the bosonic isotope ^{39}K to be $a(^{39}\text{K}) \equiv a_b = 4.3$ (nm) with corresponding cross section $\sigma_{bb} = 8\pi^2 a_b^2$ and the s -wave scattering length between ^{39}K and the fermionic isotope ^{40}K to be $a(^{40}\text{K} - ^{39}\text{K}) \equiv a_{bf} = 2.5$ (nm) with cross section $\sigma_{bf} = 4\pi^2 a_{bf}^2$ [24]. Using $M(^{40}\text{K}) = 6.6 \times 10^{-26}$ kg and $\omega = 400$ (Hz) sets the time scale $\tau_0 = 1254$ (s) ≈ 20 (min). Mean-field effects become important when the mean-field strength $E_{\text{mean}} = [4\pi\hbar^2 a_b / M(^{40}\text{K})] \bar{n}_0$ is of the order of the level spacing $\hbar\omega$ [25]. At the onset of BEC the density pro-

file of an ideal Bose gas is almost Gaussian and the mean density of the ground state becomes $\bar{n}_0 = N_0 / \pi^{3/2} l^3$. The ratio of the mean-field strength to the trap energy is then

$$\gamma = \frac{E_{\text{mean}}}{\hbar\omega} = \sqrt{\frac{1}{\pi}} \frac{a_b}{l} N_0 = 1.72 \times 10^{-3} N_0. \quad (22)$$

Further discussions of the influence of mean-field effects on our results is given below. In Figs. 8 and 9 we present an example of evaporative cooling for a spin-polarized $^{40}\text{K} - ^{39}\text{K}$ mixture of 10^6 bosons and 10^5 fermions at initial temperatures $T_b = T_C = 0.3$ (μK) and $T_f = 7.2 T_F = 1.8$ (μK) and cutoff energy $E_{\text{cut}}(0) = 1000$. We estimate the boson scattering rate using Eq. (15), which yields $\approx 5 \times 10^3 / \tau_0$. From $\tau = 0$ until $\tau = 0.04$ the cutoff energy remains at $E_{\text{cut}} = 1000$. During the thermalization the Bose distribution completely

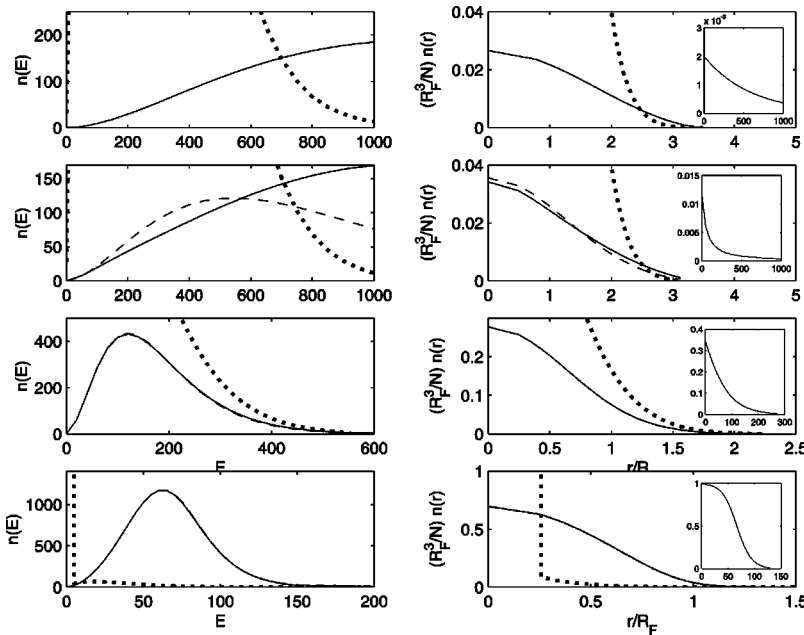


FIG. 8. Sympathetic cooling of the fermionic potassium isotope ^{40}K by the bosonic isotope ^{39}K . The Fermi (solid line) and Bose (dotted line) distribution functions at times $\tau = 0, 3.6 \times 10^{-4}, 4.7 \times 10^{-2},$ and 6.1×10^{-2} . The graphs on the left show the number of atoms as a function of energy, the graphs on the right show the spatial distribution, and the inset shows the number of fermions per energy divided by the degeneracy. Initial conditions are $N_b(0) = 10^6, N_f(0) = 10^5, \bar{T}_b(0) = \bar{T}_C = 94.1, \bar{T}_f(0) = 7.2 \bar{T}_F = 590.4$. From $\tau = 0$ until $\tau = 0.04$ the cutoff for both gases $E_{\text{cut}} = 1000$. After $\tau = 0.04$ the cutoff energy is ramped down with a rate $\gamma = 100.0$. The broken line denotes the fit to the Fermi distribution. The Fermi gas temperatures from top to bottom are $\bar{T}_f(\tau) = 7.2 \bar{T}_F, 1.62 \bar{T}_F, 0.67 \bar{T}_F,$ and $0.14 \bar{T}_F$. The Bose temperature is $\bar{T}_b(\tau) = \bar{T}_C, 1.02 \bar{T}_C, 0.63 \bar{T}_C,$ and $0.12 \bar{T}_C$.

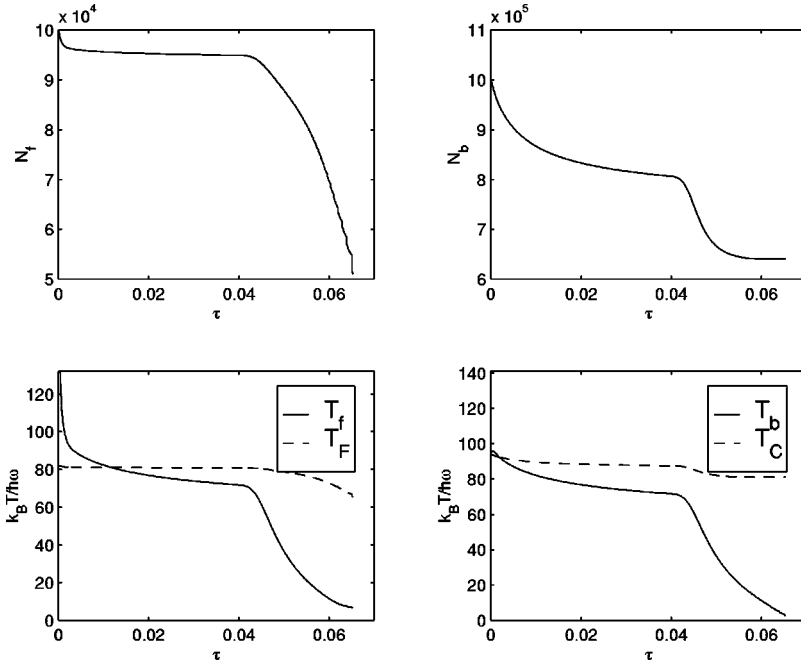


FIG. 9. Upper graph: the number of bosons and fermions remaining in the trap. Lower graph: the temperature of the gases as a function of time. The dashed lines show the critical temperature for the Bose gas and the Fermi temperature.

envelops the Fermi distribution, which deviates significantly from its equilibrium distribution. As one can see from Fig. 9, the number of fermions almost remains the same whereas a large number of bosons are evaporated. After $\tau=0.04$, the cutoff energy is ramped down exponentially with rate $\gamma_{\text{evap}} = 100/\tau_0$ until $\tau=0.064 \cong 80.25$ (s). At the early stages of the forced evaporation the number of bosons decreases until most of the bosons are in the condensate and evaporation mainly leads to depletion of fermions. The simulation shows that the Fermi gas can be cooled to a temperature $T_f \approx 0.1T_F$ with more than 2×10^4 fermions left in the trap.

In practice there are some additional issues that must be considered. The isotopes have different mass and magnetic moment, which means that in general the clouds will be displaced with respect to one another due to the combined effects of gravity and the magnetic trapping force [3]. Sympathetic cooling can only proceed efficiently if good overlap between the gases is maintained [26,27] and effects of superfluidity can be ignored [28]. Even if we assume this has been achieved, the difference in magnetic moments will cause the trap frequencies to be different for the Bose and Fermi gas. For example, if the bosonic ^{39}K ($I=7/2$, where I , is the nuclear spin) is polarized in the state $|F=2, M_F=2\rangle$, and the fermion isotope ^{40}K ($I=4$) is polarized in the state $|F=7/2, M_F=-7/2\rangle$, the trap frequencies would be in the ratio of 7:9. In our calculation we assume the trap frequencies and masses to be identical.

For degenerate Bose and Fermi gases, mean-field effects can strongly influence the spatial distributions. Here we discuss how these effects qualitatively change the stationary distributions presented above, using the zero-temperature model discussed by Mølmer [12]. If the number of bosons is much larger than the number of fermions, then as a_{bf} increases relative to a_b ($a_{bf}, a_b > 0$), the fermion distribution is displaced further and further outside of the central core of the trap occupied by the bosons. When the particle numbers are similar, the bosons are displaced outside the fermion region in the same limit. On the other hand, for large negative

fermion-boson scattering length the stationary distributions may be unstable and dynamically change as a result. In the latter case, mean-field effects qualitatively change the nature of the problem, and thus our results will not apply.

In our simulations the number of bosons is always much larger than the number of fermions. In this case we can neglect to first order the influence of the fermions on the boson spatial distribution. The boson density is then given by the Thomas-Fermi approximation

$$n_b(\vec{r}) = [\mu - V_{\text{ext}}(\vec{r})]/a_b, \quad (23)$$

where $V_{\text{ext}}(\vec{r}) = M\omega^2 r^2/2$ denotes the harmonic trapping potential and the chemical potential μ is fixed through the condition $\int d\vec{r} n_b(\vec{r}) = N_b$. Explicitly, this yields

$$\mu = \left[\left(\frac{m\omega^2}{2} \right)^{3/2} \frac{15}{8\pi} N_b a_b \right]^{2/5}. \quad (24)$$

The bosonic mean field produces the well known broadening of the boson density distribution relative to the ground-state size of the trap. The corresponding spatial distribution of fermions can be found from the equation [12]

$$\frac{\hbar^2}{2M} [6\pi^2 n_f(\vec{r})]^{2/3} + \left(1 - \frac{a_{bf}}{a_b} \right) V_{\text{ext}}(\vec{r}) + \frac{a_{bf}}{a_b} \mu = E_F, \quad (25)$$

where E_F is determined by $\int d\vec{r} n_f(\vec{r}) = N_f$. Explicitly the density is given by

$$n_f(r) = \frac{N_f}{R_F^3} \frac{8}{\pi^2} \left[1 - \frac{a_{bf}}{a_b} \frac{\mu}{E_F} - \left(1 - \frac{a_{bf}}{a_b} \right) \left(\frac{r}{R_F} \right)^2 \right]^{3/2} \quad (26)$$

which may be compared with Eq. (21) for an ideal gas. Clearly the mean-field effects cause a broadening in the spatial distribution of the fermion cloud for $a_{bf} < a_b$. If $a_{bf} > a_b$, the fermions experience an inverted harmonic-

oscillator potential near the origin which repels them from this region. In our results presented above, and in particular for the example of the potassium isotopes, we always have $a_{bf} < a_b/2$. As a result, mean-field effects will result in a broadening of both Bose and Fermi gas spatial distributions, but not a relative displacement of the clouds.

V. CONCLUSION

We have discussed the cooling of a confined nondegenerate Fermi gas to quantum degeneracy using an ultracold Bose gas coolant and evaporative cooling. Results for the stationary distributions and dynamics based on solutions of

coupled QBE equations for the Bose-Fermi mixture were presented. These include investigations of the use of forced evaporative cooling to enhance the degeneracy of the Fermi gas. While the QBE does not include mean-field effects, which are potentially important in the quantum degenerate regime, we have discussed their qualitative effects on the results presented, when $a_b > a_{bf} > 0$. In this instance, mean fields lead to a broadening of both the Bose and Fermi spatial distributions, but not a relative displacement of the clouds.

ACKNOWLEDGEMENTS

We acknowledge support from the NSF and ONR.

-
- [1] M. H. Anderson, J. R. Ensher, M. R. Matthews, C. E. Wieman, and E. A. Cornell, *Science* **269**, 198 (1995); K. B. Davis, M.-O. Mewes, M.R. Andrews, N. J. van Druten, D. S. Durfee, D. M. Kurn, and W. Ketterle, *Phys. Rev. Lett.* **75**, 3969 (1995); C. C. Bradley, C. A. Sackett, J. J. Tollet, and R. G. Hulet, *ibid.* **75**, 1687 (1995); **79**, 1170 (1997).
- [2] For an extensive list of references, see the BEC on-line bibliography maintained by M. Edwards at <http://amo.phy.gasou.edu/bec.html/bibliography.html>.
- [3] C. J. Myatt *et al.*, *Phys. Rev. Lett.* **78**, 586 (1997); D. S. Hall, M. R. Matthews, J. R. Ensher, C. E. Wieman, and E. A. Cornell, *ibid.* **81**, 1539 (1998).
- [4] J. Stenger, S. Inouye, D. M. Stamper-Kurn, H.-J. Miesner, A. P. Chikkatur, and W. Ketterle, *Nature (London)* (to be published).
- [5] F. S. Cataliotti, E. A. Cornell, C. Fort, M. Inguscio, F. Marin, M. Prevedelli, L. Ricci, and G. M. Tino, *Phys. Rev. A* **57**, 1136 (1998).
- [6] H. T. C. Stoof, M. Houbiers, C. A. Sackett, and R. G. Hulet, *Phys. Rev. Lett.* **76**, 10 (1996); M. Houbiers, R. Ferwerda, H. T. C. Stoof, W. I. McAlexander, C. A. Sackett, and R. G. Hulet, *Phys. Rev. A* **56**, 4864 (1997); M. Houbiers and H. T. C. Stoof, *Phys. Rev. A* **59**, 1556 (1998).
- [7] E. R. I. Abraham, W. I. McAlexander, J. M. Gerton, R. G. Hulet, R. Cote, and A. Dalgarno, *Phys. Rev. A* **55**, R3299 (1997); M. Houbiers, H. T. C. Stoof, W. I. McAlexander, and R. G. Hulet, *ibid.* **57**, R1497 (1998).
- [8] J. Schneider and H. Wallis, *Phys. Rev. A* **57**, 1253 (1998).
- [9] M. A. Baranov, Yu. Kagan, and M. Yu. Kagan, *JETP Lett.* **64**, 301 (1996); M. A. Baranov and D. S. Petrov, *Phys. Rev. A* **58**, 801 (1998); M. A. Baranov, e-print cond-mat/9801142 (unpublished).
- [10] B. DeMarco and D. S. Jin, *Phys. Rev. A* **58**, 801 (1998).
- [11] Millions of ^{82}Rb atoms have been trapped and cooled by Dr. Vieira's group at the Los Alamos National Laboratory. A similar technique can also be applied to ^{84}Rb and ^{86}Rb atoms. R. Guckert, X. Zhao, S. G. Crane, A. Hime, W. A. Taylor, D. Tupa, D.J. Vieira, and H. Wollnik, *Phys. Rev. A* **58**, R1637 (1998).
- [12] K. Mølmer, *Phys. Rev. Lett.* **80**, 1804 (1998).
- [13] D. W. Snoke and J. P. Wolfe, *Phys. Rev. B* **39**, 4030 (1988).
- [14] O. J. Luiten, M. W. Reynolds, and J. T. M. Walraven, *Phys. Rev. A* **53**, 381 (1996).
- [15] M. Holland, J. Williams, and J. Cooper, *Phys. Rev. A* **55**, 3670 (1997).
- [16] Huang Wu, Ennio Arimondo, and Christopher J. Foot, *Phys. Rev. A* **56**, 560 (1997).
- [17] E. L. Surkov, J. T. M. Walraven, and G. V. Shlyapnikov, *Phys. Rev. A* **53**, 3403 (1996).
- [18] D. A. Butts and D. S. Rokhsar, *Phys. Rev. A* **55**, 4346 (1997).
- [19] T. Lopez-Arias and A. Smerzi, *Phys. Rev. A* **58**, 526 (1998).
- [20] J. R. Anglin, J. P. Paz, and W. H. Zurek, *Phys. Rev. A* **55**, 4041 (1997).
- [21] W. Geist, T.A.B. Kennedy, and L. You (unpublished).
- [22] D. Jaksch, C. W. Gardiner, and P. Zoller, *Phys. Rev. A* **56**, 575 (1997).
- [23] M. Edwards and K. Burnett, *Phys. Rev. A* **51**, 1382 (1995).
- [24] R. Cote, A. Dalgarno, H. Wang, and W. C. Stwalley, *Phys. Rev. A* **57**, R4118 (1998).
- [25] K. G. Singh and D. S. Rokhsar, *Phys. Rev. Lett.* **77**, 1667 (1996).
- [26] W. Ketterle and N. J. van Druten, in *Advances in Atomic, Molecular and Optical Physics*, edited by B. Bederson and H. Walther (Academic Press, San Diego, 1996), Vol. 37, p. 181.
- [27] M. Amoruso, A. Minguzzi, S. Stringani, M. P. Tosi, and L. Vichi, e-print cond-mat/9810210.
- [28] Eddy Timmermans and R. Côté, *Phys. Rev. Lett.* **80**, 3419 (1998).